PERGAMON

International Journal of Solids and Structures 37 (2000) 311–329

INTERNATIONAL JOURNAL OF SOLIDS and STRUCTURES

www.elsevier.com/locate/ijsolstr

Mechanics and mechanisms of fatigue damage and crack growth in advanced materials

R.O. Ritchie*, C.J. Gilbert, J.M. McNaney

Materials Sciences Division, Lawrence Berkeley National Laboratory and Department of Materials Science and Mineral Engineering, University of California, 463 Evans Hall #1760, Berkeley, CA 94720-1760, USA

Abstract

The mechanisms of fatigue-crack propagation in ceramics and intermetallics are examined through a comparison of cyclic crack-growth behavior in ductile and brittle materials. Crack growth is considered to be a mutual competition between *intrinsic* mechanisms of crack advance ahead of the crack tip, which promote crack growth, and *extrinsic* mechanisms of crack-tip shielding behind the tip, which impede it. In this paper, we examine and model the widely differing nature of these mechanisms, with emphasis on behavior in ceramics at ambient and elevated temperatures, and compare their specific dependencies upon the alternating and maximum driving forces (e.g., ΔK and K_{max}), thereby providing a useful distinction of the process of fatigue-crack propagation in these different classes of materials. Published by Elsevier Science Ltd.

Keywords: Fatigue-crack growth; Crack-tip shielding; Ceramics; Intermetallics

1. Introduction

There has been increasing interest in the use of high-strength, brittle materials, such as ceramics, intermetallics and their respective composites for structural applications where cyclic loading is critical. Much of the interest has focused on elevated temperature applications, e.g., for automobile and aerospace engine components. In the case of ceramics for biomedical implant devices, however, properties at ambient temperatures are also critical. Examples are the use of Si_3N_4 ceramics for automobile turbocharger wheels and engine valves, and pyrolytic carbon for prosthetic cardiac devices. Similarly, intermetallic alloys, such as the γ-based titanium aluminides, have also been considered for automobile engine valves and gas-turbines blades. Whereas these materials offer vastly improved specific strength at high temperatures compared to conventional metallic alloys, they suffer from a pronounced

* Corresponding author Tel.: +1-510-486-5798; fax: +1-510-486-4995.
E-mail address: roritchie@lbl.gov (R.O. Ritchie)

0020-7683/00/$ - see front matter. Published by Elsevier Science Ltd.
PII: S0020-7683(99)00096-7

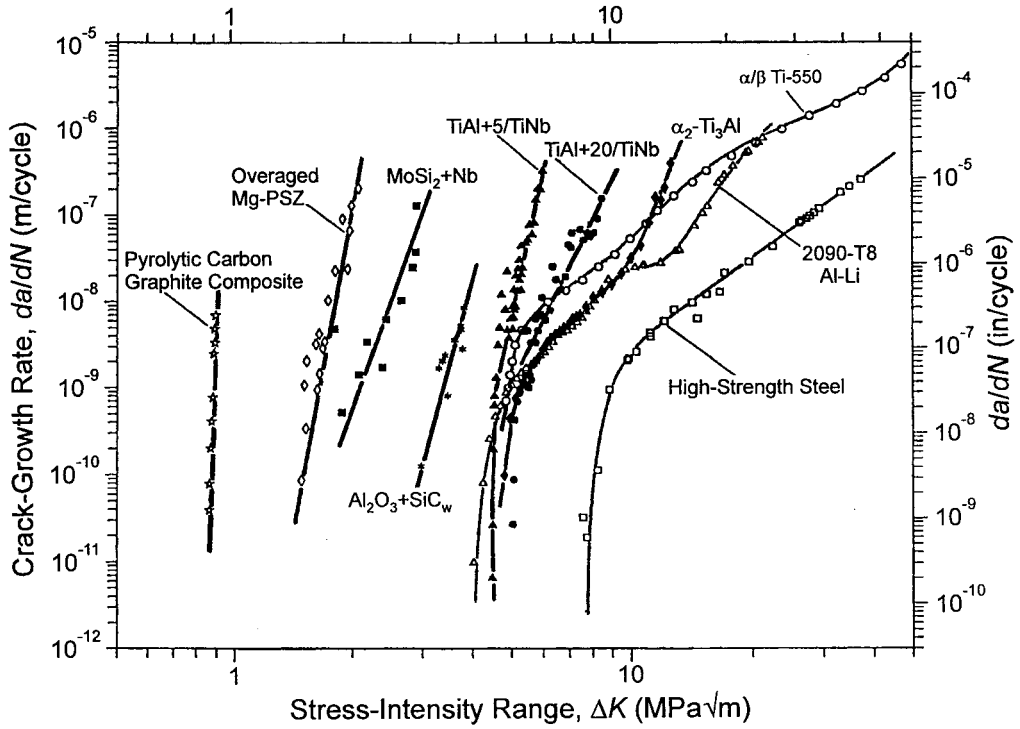

Fig. 1. Variation of fatigue-crack propagation rates (da/dN) with applied stress intensity range (ΔK), for metals, intermetallics and ceramics.

lack of damage tolerance. Moreover, it is now known that they are susceptible to cyclic fatigue failure (e.g., Dauskardt et al., 1987). Ironically, this fatigue susceptibility increases in microstructures designed for greater damage tolerance.

In brittle materials, such as monolithic and composite ceramics and intermetallics, the mechanisms associated with fatigue-crack propagation are quite distinct from those encountered in metal fatigue.

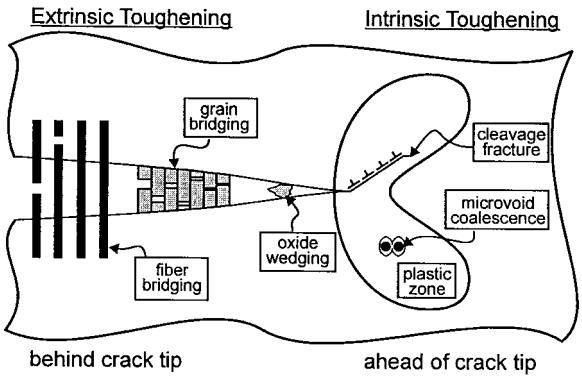

Fig. 2. Schematic illustration of mutual competition between intrinsic mechanisms of damage/crack advance and extrinsic mechanisms of crack-tip shielding involved in crack growth.

The sensitivity of crack-growth rates, da/dN, to the applied stress intensity, K, for example, is markedly higher than in most metals (Fig. 1). The notion that crack growth is a mutual competition between *intrinsic* microstructural damage mechanisms and *extrinsic* crack-tip shielding mechanisms provides a useful framework to compare fatigue mechanisms of ductile and brittle materials (Ritchie, 1988). Intrinsic mechanisms are defined as those which promote crack extension via processes at or ahead of the crack tip, while extrinsic mechanisms operate behind the crack tip and typically retard crack growth.

In this paper, the fatigue of ceramics and intermetallics is briefly described by examining the commonality of mechanisms affecting fatigue-crack growth in ductile and brittle materials, with particular focus on the role of these intrinsic and extrinsic processes.

2. Intrinsic and extrinsic mechanisms

Resistance to crack extension results from a competition between two classes of mechanisms (Fig. 2). Crack growth is promoted *ahead* of the crack tip by *intrinsic* microstructural damage mechanisms, and impeded by *extrinsic* mechanisms acting primarily *behind* the crack tip, which serve to screen the crack tip from the far-field driving force. In metals, intrinsic damage mechanisms under cyclic loading typically involve blunting and resharpening of the crack. Extrinsic shielding mechanisms, conversely, result from the creation of inelastic zones surrounding the crack wake or from physical contact between the crack surfaces via wedging, bridging, sliding or combinations thereof (Ritchie, 1988). Examples of 'zone shielding' are transformation and microcrack toughening in ceramics. Examples of 'contact shielding' are the bridging tractions imposed across a crack by unbroken fibers, laminated layers or a particulate phase in composites (Evans, 1990), or the wedging of corrosion debris or fracture surface asperities in metal fatigue (referred to as crack closure).

Intrinsic mechanisms are an inherent property of the material, and thus are active irrespective of crack size or geometry. They control driving forces (or stress intensities) necessary to *initiate* cracking. Extrinsic mechanisms, conversely, act in the crack wake and are thus dependent on crack size and specimen geometry. They are responsible for resistance-curve (R-curve) behavior and consequently play a prominent role in the driving forces required for continued *growth* of the crack. Thus, where extrinsic shielding mechanisms are active, rising R-curve toughness behavior and 'small-crack' effects are to be expected. Moreover, since extrinsic mechanisms have little effect on crack initiation, the microstructural factors affecting crack growth (when cracks are large and possess a fully developed wake) may be quite different from those affecting crack initiation (when cracks are small and possess no wake).

Dominant toughening mechanisms in ductile materials are intrinsic, e.g., mobile dislocation activity and the associated crack-tip plasticity (although under cyclic loads extrinsic mechanisms play a critical role in the form of crack closure). In contrast, brittle materials are invariably toughened extrinsically. Examples include transformation toughening and crack bridging, the latter through interlocking grains in monolithic ceramics or by intact reinforcement phases in composites and laminates (e.g., Evans, 1990). From the perspective of fatigue-crack growth, *it is the specific nature and, more significantly, the relative importance of the intrinsic (damage) versus extrinsic (shielding) mechanisms which distinguishes the fatigue behavior of ductile and brittle solids*. This, in turn, governs the specific dependencies of crack-growth rates on ΔK and K_{max} (Dauskardt et al., 1992).

3. Fatigue-crack propagation in ceramics

3.1. Behavior at ambient temperatures

Intrinsic toughening mechanisms have been largely unsuccessful in glasses and ceramics. Rather,

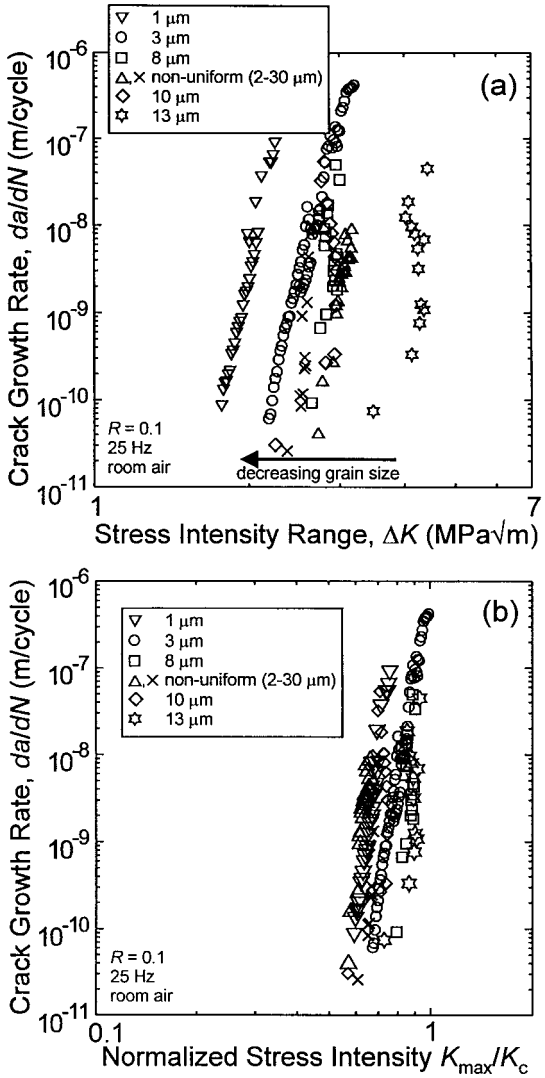

Fig. 3. Fatigue-crack growth rates, da/dN, as a function of a) the applied stress-intensity range, ΔK, and b) the maximum stress intensity normalized by the fracture toughness, K_{max}/K_c, for a range of polycrystalline aluminas (Gilbert and Ritchie, 1997).

ceramic materials are toughened using various extrinsic shielding mechanisms. They can now be processed with up to an order of magnitude higher toughness than was available ~20 years ago (Evans, 1990). It is ironic that whereas glasses and untoughened ceramics are essentially immune to cyclic fatigue, these newly-developed damage tolerant microstructures are quite prone to cycle-dependent failures. The introduction of crack-wake shielding and other energy-absorbing processes have introduced microstructural features prone to cyclic damage. As one might expect, the characteristics of ceramic fatigue are quite different from those of metal fatigue:

1. Unlike ductile materials [with the exception of phase-transforming ceramics such as PSZ (Steffen et al., 1991)], fatigue cracks in ceramics do not appear to initiate naturally. Rather, crack initiation is invariably associated with some pre-existing defect.

2. Again, unlike metal fatigue where striation growth is the characteristic fatigue fracture mode, the morphology of fatigue fracture surfaces in ceramics is almost identical to that under monotonic loads (although wear debris is often present) (Dauskardt et al., 1992; Gilbert et al., 1996; Gilbert and Ritchie, 1997; Liu and Chen, 1991; Lathabai et al., 1988).
3. Microstructure has a significant effect on fatigue-crack growth rates in ceramics. A striking example is the variation in da/dN with ΔK for a series of aluminas with increasing toughness (associated with an increase in grain size from ~1 to 30 μm). By normalizing the data in terms of the toughness, i.e., by plotting in terms of K_{max}/K_c, the microstructural effects are essentially normalized (Fig. 3) (Gilbert and Ritchie, 1997). This implies that unlike metals, the microstructural influences in ceramics on fatigue fracture are similar to those for static fracture.
4. The sensitivity of growth rates to the stress intensity is extremely high in ceramics. The exponent m in the simple Paris equation ($da/dN \propto \Delta K^m$) can take values as high as ~15 to 50 and above (Fig. 1). Such high exponents result from a marked sensitivity of growth rates to K_{max}, rather than to ΔK. This is appreciated by expressing the growth-rates in terms of both K_{max} and ΔK, viz (Dauskardt et al., 1992; Liu and Chen, 1991):

$$\frac{da}{dN} = C'(K_{max})^n(\Delta K)^p, \tag{1}$$

where C' is a scaling constant and $(n+p)=m$. In ceramics, $p \ll n$, e.g., for toughened SiC, $n = 36$ and $p = 1.9$ (Gilbert et al., 1996), whereas in metals, $n \ll p$, e.g., for a Ni-base superalloy, $n = 0.5$ and $p = 3$ (Van Stone, 1988); in intermetallics $n \sim p$.

Fatigue can be considered either in terms of the accumulation of distributed damage or as the propagation of a single dominant crack. In the former case, this has been studied in terms of contact fatigue under repeated indentation (Lawn, 1998), where damage is associated with a diffuse zone of microcracks under the indenter. Here failure proceeds by the growth and coalescence of microcracks, rather than in the latter case by the extension of a single crack to some critical size. At a microstructural level, however, the mechanisms are quite similar. Contact fatigue is modeled as distributed frictional damage along grain-boundary shear faults, whereas the fatigue of a single dominant crack is modeled as frictional damage at grain-bridging sites behind the crack tip.

For fatigue-crack propagation of a single crack, there are two possible classes of fatigue mechanisms:

1. *intrinsic mechanisms* where, as in metals, crack advance results from damage processes in the crack-tip region, which are unique to cyclic loading, and
2. *extrinsic mechanisms*, where the crack-advance mechanism ahead of the crack tip is identical to that for monotonic loading, but the unloading cycle promotes accelerated crack growth by degrading crack-tip shielding behind the tip (Ritchie, 1988).

Whereas the cyclic processes in metal fatigue are predominantly intrinsic in nature, cyclic fatigue processes in ceramics are extrinsic. This is consistent with the marked dependency of growth rates on K_{max} in ceramics and a similarity in fracture surface appearance under cyclic and monotonic loading. Specifically, cyclic loading acts to diminish shielding (i.e., R-curve toughening) in the crack wake (Lathabai et al., 1988; Dauskardt and Ritchie, 1993; Dauskardt, 1993; Kishimoto et al., 1995; Gilbert and Ritchie, 1998). This can take various forms depending upon the prevailing shielding mechanism. Examples include premature fatigue failure of metallic reinforcement phases in ductile-phase toughened materials (Venkateswara Rao et al., 1994), a reduction in the effect of fiber bridging in fiber-reinforced composites (Rouby and Reynaud, 1993), and a decreased bridging capacity of interlocking grains in grain-bridging ceramics, such as coarse-grained Al_2O_3, and grain-elongated Si_3N_4 and SiC (Gilbert et al., 1996, 1995; Gilbert and Ritchie, 1998).

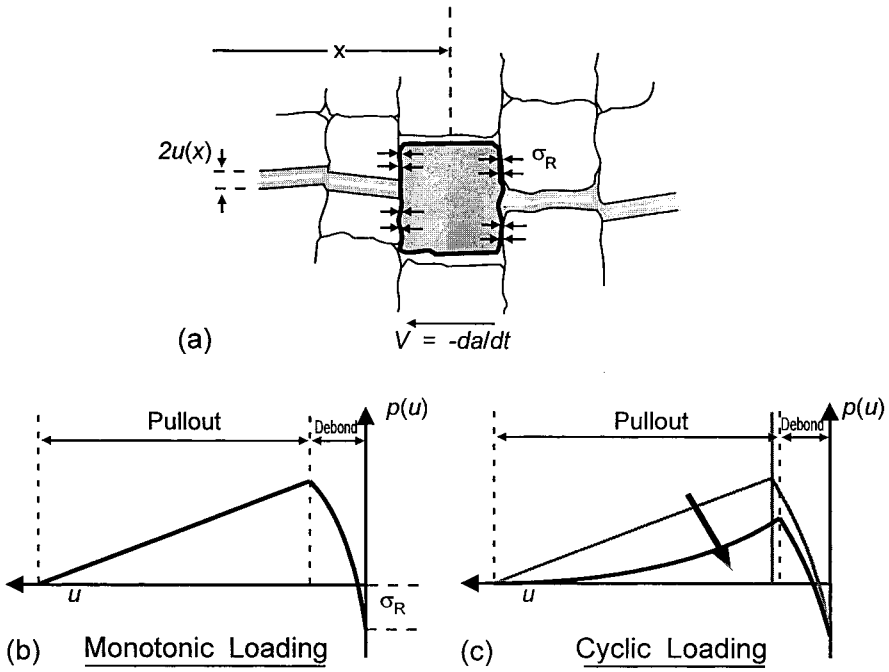

Fig. 4. Schematic illustration of the frictional wear model for ambient temperature fatigue-crack growth, showing (a) a grain bridge in the wake of a growing crack. The grain-bridging stress, $p(u)$, rises from the initial residual compressive stress, σ_R, as the grain debonds, followed by frictional sliding which gradually decreases as the grain is pulled out from the matrix, under (b) monotonic and (c) cyclic loading conditions.

3.1.1. Grain bridging

To illustrate this phenomenon, the latter mechanism of fatigue-degradation operating in monolithic ceramics is considered (Lathabai et al., 1988; Dauskardt and Ritchie, 1993; Dauskardt, 1993; Kishimoto et al., 1995; Gilbert and Ritchie, 1998; Venkateswara Rao et al., 1994; Rouby and Reynaud, 1993; Gilbert et al., 1995; Lawn, 1993; Hay and White, 1993; Mai and Lawn, 1987; Foote et al., 1986). In this case, decay in bridging is associated with the relative motion and subsequent frictional wear of ligaments or grains spanning the crack walls (the presence of bridging elements is enhanced by elongated microstructures that exhibit intergranular failure) (Fig. 4). Under monotonic loading, the closing traction distribution associated with grain bridging, $p(x)$, has been well documented. It can be expressed most simply in terms of a bridging zone length, L, an exponent, k, and a peak bridging stress, P_{max}, as (e.g., Lawn, 1993; Hay and White, 1993; Mai and Lawn, 1987; Foote et al., 1986):

$$p(x) = P_{max}(1 - x/L)^k. \tag{2}$$

The function $p(x)$ describes the bridging stress distribution as a function of distance behind the crack tip, x, starting from a maximum value of P_{max} at the crack tip ($x = 0$), and falling to zero at the end of the bridging zone ($x = L$). This drop in bridging tractions with x is characteristic of frictional bridging. The shape of the decrease is determined by the exponent k; a uniformly distributed stress over the bridging zone would imply $k = 0$, whereas $k = 1$ corresponds to frictional pullout where the cross-sectional geometry of the bridging grains does not change during crack opening. Note that this simplification ignores any initial rising portion of the curve that may be associated with grain-debonding

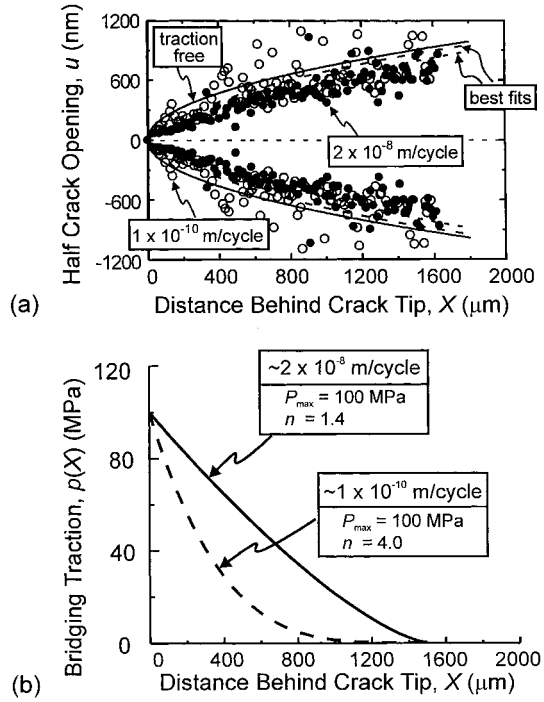

Fig. 5. Measured crack-opening profiles in ABC–SiC for (a) Case I where the crack was grown near instability at ~92% K_c, and Case II where the crack was grown near threshold at ~75% K_c. In (b), the best-fit bridging traction distributions are plotted for each case (Gilbert and Ritchie, 1998).

or elastic bridging. The energy absorbed by these processes is typically much smaller than frictional pullout, and so for our purposes it is neglected.

Under cyclic loads, the repetitive opening and closing of the crack results in a decrease in the toughening capacity of the bridging zone by reducing the grain bridging stress. Accumulated frictional-wear damage at the grain/matrix interface and the accompanying reduced frictional sliding resistance of partially debonded grains reduces frictional pullout stresses, lowers closing tractions, and elevates crack-growth rates under cyclic loading.

Bridging-traction distributions under specified loading conditions can be quantified by comparing measured crack-opening profiles, $u(x)$, to known elastic solutions for bridged cracks [e.g., the well-known Barenblatt solution (Barenblatt, 1962)], using a method first suggested by Rödel et al. (1990). The net crack-opening profile, $u(x)$, for a linear-elastic crack under an applied far-field stress intensity, K_A, with a bridging traction distribution, $p(x)$, of length L acting across the crack faces can be expressed, in terms of the appropriate elastic modulus E', as:

$$u(x) = \frac{K_A}{E'}\left(\frac{8x}{\pi}\right)^{\frac{1}{2}} + \frac{2}{\pi E'}\int_0^L p(x')\ln\left|\frac{\sqrt{x'}+\sqrt{x}}{\sqrt{x'}-\sqrt{x}}\right| dx'. \tag{3}$$

The first term in Eq. (3) reflects the *traction free* crack under tensile loading in small-scale yielding (Irwin, 1958), and the second term accounts for contributions associated with the traction-stress distribution. Because Eq. (3) is the near-tip solution and neglects specimen boundary or geometry

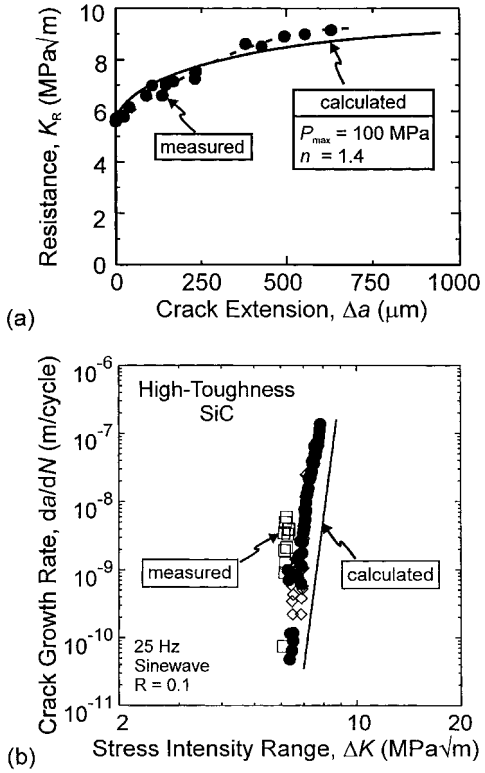

Fig. 6. Crack opening profile measurements in Fig. 5 were used to simulate (a) the resistance curve, and (b) the cyclic fatigue-crack growth rates in ABC–SiC (Gilbert and Ritchie, 1998).

effects, this description is only sufficient when bridging zones are small compared to specimen size and crack length.

Using this technique, the extrinsic mechanism for fatigue-crack growth described above has been verified experimentally. Crack-opening profiles (and so their accompanying bridging traction distributions) of cracks grown near the fracture instability (to simulate behavior on the R-curve) were compared to cracks grown at near-threshold growth rates (to generate a cyclically loaded crack with a degraded bridging zone). Measurements of the crack-opening profile on a high-toughness silicon carbide (Gilbert and Ritchie, 1998), loaded in the SEM to $K_A = 6.22$ MPa m^{-2}, are plotted in Fig. 5(a) for a crack grown at ~92% K_c (Case I). Also shown are the best-fit profile determined from Eq. (3) (dashed line) and the calculated opening profile for a traction-free crack (solid line). The bridging distribution can be estimated using Eq. (3), and fitting to the form of $p(x)$ described in Eq. (2). Once $p(x)$ is determined, it is possible to calculate the associated R-curve and compare it to experimental measurements [Fig. 6(a)]. The R-curve is calculated via (Lawn, 1993):

$$K_B(\Delta a) = \left(\frac{2}{\pi}\right)^{\frac{1}{2}} \int_0^{\Delta a} \frac{p(x)}{\sqrt{x}}\, dx, \tag{4}$$

where K_B is the bridging term and Δa is the amount of crack extension. By varying Δa from $\Delta a = 0$ to $\Delta a = L$, the resistance curve, $K_R(\Delta a)$, can be determined from:

$$K_R(\Delta a) = K_0 + K_B(\Delta a), \tag{5}$$

where K_0 is the long-crack initiation toughness ($\sim$5.5 MPa m^{-2} for this SiC). Predictions (Gilbert and Ritchie, 1998) shown in Fig. 6(a), are in reasonable agreement with those measured experimentally (Gilbert et al., 1996) on compact-tension specimens.

The corresponding opening profile (at $K_A = 6.22$ MPa m^{-2}) for a crack grown after extensive fatigue cycling at a near-threshold growth rate of $\sim 1 \times 10^{-10}$ m/cycle (Case II) is also shown in Fig. 5(a). It is apparent that the near-threshold crack is significantly more open than the crack grown near instability, and that it indeed approaches the profile of the traction-free crack. This is consistent with a reduction in the magnitude of bridging tractions for a bridging zone that has experienced $\sim 10^8$ loading cycles. Best-fit $p(x)$ functions from the fatigue and near-instability cracks are compared in Fig. 5(b), and show that continued cyclic loading acts to degrade the bridging tractions (Gilbert and Ritchie, 1998).

By estimating the bridging tractions at several applied K levels, the cyclic crack growth-rate data can be simulated based on the notion that the crack-advance mechanism does not change and that the influence of the cyclic loads is solely to progressively degrade crack bridging. The predicted variation in da/dN with ΔK for this SiC can be seen in Fig. 6(b) to be in reasonable agreement with experimentally measured data at a load ratio (ratio of the minimum to the maximum load) of $R = 0.1$ (Gilbert and Ritchie, 1998). The closeness of this fit, in addition to the direct quantitative evidence of cycle-induced degradation in shielding, imply that the essential physics of the cyclic-crack growth process involves cycle-dependent degradation of an active bridging zone.

3.2. Behavior at elevated temperatures

There are far fewer studies on fatigue-crack growth in ceramics at elevated temperatures (Ramamurty et al., 1994; Huang and Shang, 1995; Liu and Chen, 1996; Han and Suresh, 1989; Ewart and Suresh, 1992; Ueno et al., 1992; Ueno et al., 1993; Kishimoto et al., 1992; Ziegler et al., 1998). This is associated in part with experimental difficulties encountered at temperatures above $\sim$1000°C. More importantly, however, mechanistic interpretation is considerably more complex due to the appearance of creep damage mechanisms (e.g., grain-boundary cavitation) (Wilkinson and Vitek, 1982), thermally activated crack growth, and additional crack-tip shielding mechanisms such as viscous phase bridging (Dey et al., 1995; Ramamurty, 1996). Studies (Ziegler et al., 1998) on a near commercial silicon nitride (NT 164) reveal a small acceleration in growth rates at 800°C (where creep damage is negligible). Presumably this is due to a reduction in grain bridging caused by relaxation of the residual stresses (associated with thermal expansion anisotropy). Between 900° and 1200°C, relaxation of the bridging forces continues and so crack-growth rates are seen to increase. The acceleration is further enhanced above 1000°C with the onset of creep cavitation damage in the grain-boundary (mainly glassy) phase. Above 1200°C, the softening of the grain-boundary phase leads to an additional shielding mechanism, viscous-phase bridging, which acts to impede crack growth and to increase the tendency for crack arrest via crack-tip blunting. Moreover, the viscoelastic nature of the bridging response results in a marked dependence of crack-growth rates on loading frequency.

3.2.1. Viscous-phase bridging

As the principal shielding mechanism at elevated temperatures is such bridging, several models for viscous-phase shielding have been developed in order to predict the anticipated frequency dependence on growth rates (Dey et al., 1995; Ramamurty, 1996; McNaney et al., 1999; Yi et al., 1999). Specifically, a microstructurally-based self-consistent numerical model, which is more fully described in McNaney et al. (1999), examines in detail the mechanics of the extrinsic viscous-film bridging process (Fig. 7), with specific emphasis on its role in influencing elevated-temperature cyclic fatigue-crack propagation. The

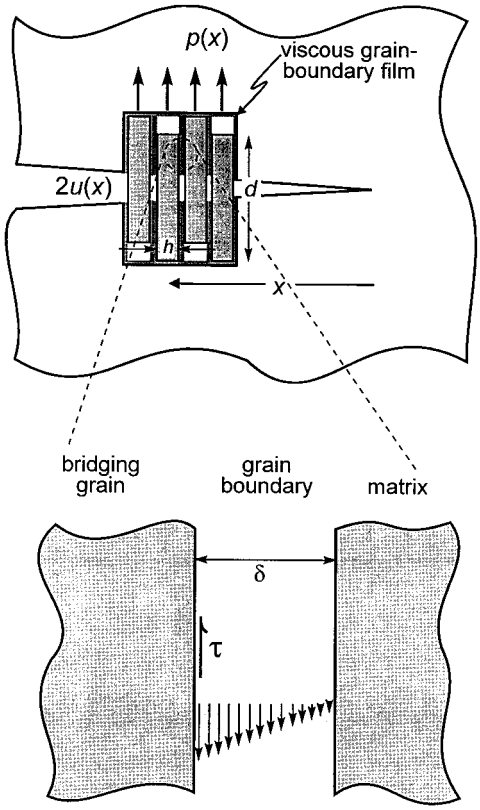

Fig. 7. Model for crack-tip shielding at higher temperatures from viscous grain-boundary film bridging, showing the development of the viscous force resulting from the velocity gradient in the film (McNaney et al., 1999).

model incorporates microstructural parameters such as grain size, viscosity and thickness of the grain-boundary film, as well as external variables such as loading frequency, cyclic load amplitude, and load ratio. Unlike previous high-temperature viscous bridging models which have presumed a parabolic crack-opening profile (Dey et al., 1995; Ramamurty, 1996), a fully self-consistent numerical approach is adopted here (no limiting assumptions are made as to the shape of the profile). Moreover, the model is not based on a viscous fluid film filling the crack (viscous-ligament bridging) (Yi et al., 1999). Rather, bridging loads are transmitted across the crack walls due to shear resistance of a grain-boundary film deforming between the matrix and the active bridging grain, allowing for the incorporation of more microstructural detail (McNaney et al., 1999). Furthermore, instead of seeking a global representation of the effect of the bridging tractions (e.g., $K_B(t)$) from a prescribed displacement distribution, the approach is to consider a displacement distribution self-consistent with the corresponding traction distribution.

The displacements due only to an arbitrary, smooth traction distribution in the wake of a crack, $u^b(x)$, are given by:

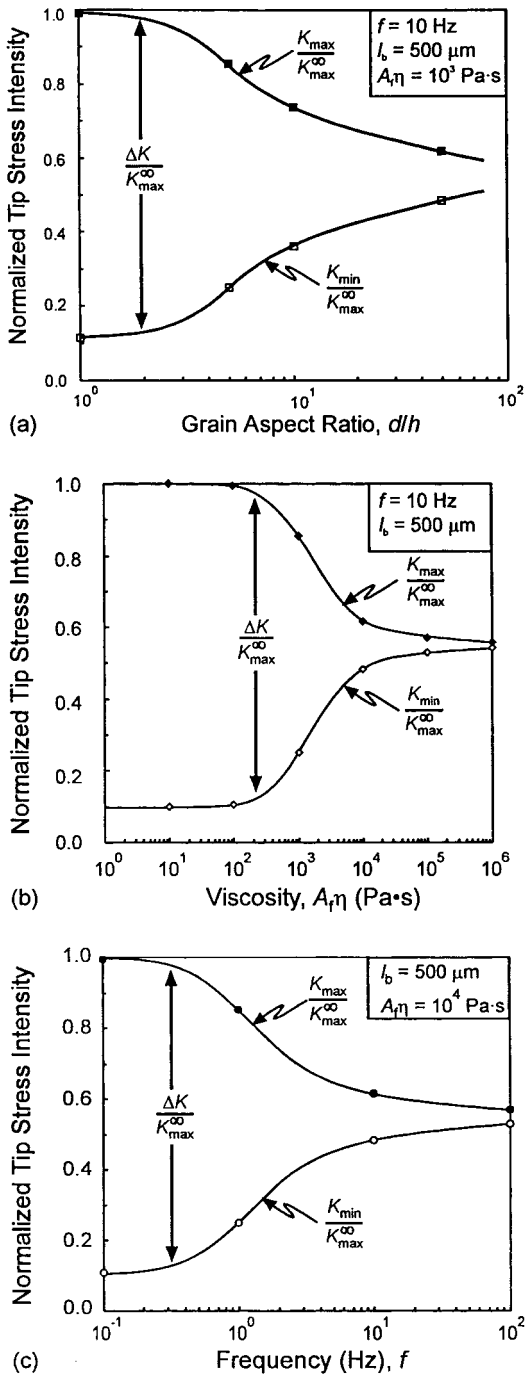

Fig. 8. Self-consistent solution results showing predicted variations in the maximum, K_{max}, and minimum, K_{min}, crack-tip stress intensity, normalized to the maximum applied stress intensity, K^{∞}_{max}, versus changes in the model parameters, namely (a) grain aspect ratio, d/h, (b) viscosity, η, and (c) frequency, f. The normalized crack-tip stress intensity range, $\Delta K/K^{\infty}_{max}$, is shown as the difference between the two curves (McNaney et al., 1999).

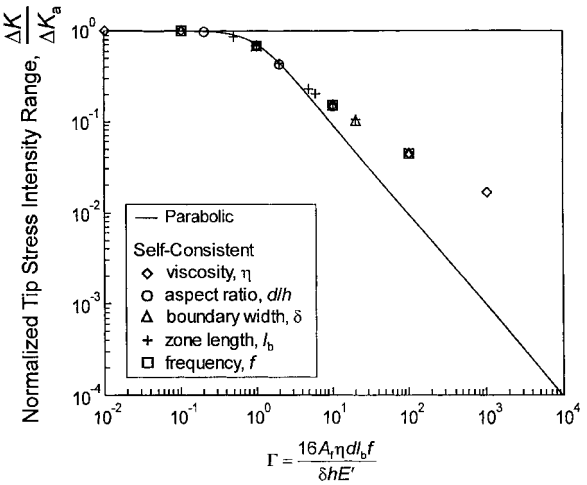

Fig. 9. Self-consistent solution results showing variations the crack-tip stress-intensity range, ΔK, normalized by the applied stress-intensity range, ΔK_a, versus the non-dimensional parameter Γ. Changes in the individual parameters of the model are shown by symbols while the parabolic solution is denoted by the solid line. Note that the self-consistent solution, which diverges from the parabolic at high Γ, is well-represented over the entire range by Γ (McNaney et al., 1999).

$$u^{b}(x) = \int_0^a \int_x^a G(\alpha,x)G(\alpha,x')p(x')\mathrm{d}\alpha\,\mathrm{d}x', \tag{6}$$

where G is the appropriate Green's function. For the self-consistent solution, where $p(x)$ is a function of $u(x)$, the following relation must be satisfied:

$$u(x) = u^{\infty}(x) + u^{b}(x), \tag{7}$$

where $u^{b}(x)$ is the contribution to the displacement from the bridging tractions, and $u^{\infty}(x)$ is the traction-free displacement distribution along the flank of the crack. The grain-boundary phase displacements are divided into elastic- and viscous-based components. The relation between these components is determined by using the equality of the elastic and viscous shear stresses in the grain-boundary phase. Although any appropriate traction-free, geometry specific, form may be used, the traction-free distribution for a semi-infinite body in plane strain is utilized (Irwin, 1958):

$$u^{\infty}(x) = \frac{K_a}{E'}\sqrt{\frac{8x}{\pi}}. \tag{8}$$

Because the displacements due to the bridging tractions depend on the total crack flank opening, a local solution along the flank of the crack is necessary in order to provide a self-consistent solution for any non-trivial problem. The methodology used in the present model provides this local solution by discretizing the crack flank and forming a pointwise solution. Where the solution between points is needed, a quadratic interpolation of the solution using the adjacent solution points is used. Furthermore, for all solutions the velocity, $\dot{u}(x)$, was approximated linearly in time.

The overall solutions allow for a complete description of the crack-opening displacements, $u(x)$, bridging stress distributions, $p(x)$, crack bridging terms, $K_B(t)$, and crack-tip loading conditions, $K_{tip}(t)$, throughout the loading history. Results from the self-consistent solutions (McNaney et al., 1999) are presented in Fig. 8 by showing changes in the normalized crack-tip loading (K_{max}/K_m, K_{min}/K_m) at steady state versus changes in the model parameters. Crack-tip shielding from bridging is seen to

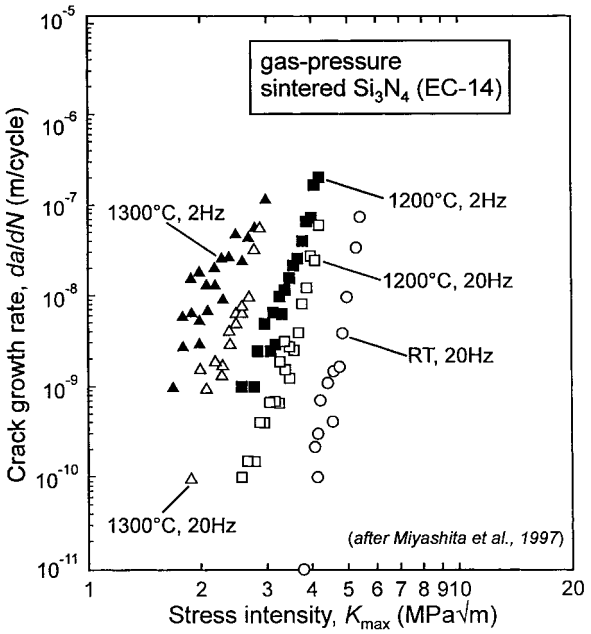

Fig. 10. Effect of cyclic frequency (2–20 Hz) on cyclic fatigue-crack growth rates, as a function of K_{max}, in gas-pressure sintered silicon nitride (EC-14) at 1200° and 1300°C, as compared to 20 Hz data at room temperature (Miyashita et al., 1998).

increase with (a) grain-aspect ratio, d/h, (b) viscosity, η, and (c) test frequency, f, for a fixed set of other parameters. Clearly, viscous-film bridging is a potentially effective shielding mechanism that can markedly reduce the stress intensity actually experienced at the crack tip during cyclic fatigue at elevated temperatures (Fig. 8).

A closed-form solution to a simplified version of the bridging model is possible when a parabolic, K_{tip}-controlled displacement distribution is assumed. This solution yields an appropriate non-dimensional group for characterizing the results of the self-consistent calculations given by:

$$\Gamma = \frac{16A_f\eta d l_b f}{\delta h E}. \tag{9}$$

where A_f is the area fraction of bridging ligaments, l_b is the bridging-zone length, E is Young's modulus, and δ is the grain-boundary width. A comparison of the trends predicted using self-consistent and parabolic solutions is presented in Fig. 9 by plotting the normalized crack-tip cyclic loading versus the non-dimensional group, Γ, which is a function of the primary model parameters. This allows a judgement to be made as to the appropriateness of Γ as a characterizing parameter. It is evident that the parameter, Γ, normalizes the results over the entire range of the parameters studied here and acts as an appropriate non-dimensional grouping. Indeed, an order of magnitude trade-off exists between the various parameters of the model. For example, an increase in the viscosity by a factor of ten would have exactly the same effect as a decrease in the frequency by a factor of ten.

Similar to the parabolic approximation, for the self-consistent solution the normalized cyclic loading rapidly changes over the range $1 < \Gamma < 100$ from full to very low transmission of the applied loading to the crack tip. At low Γ, the self-consistent and parabolic solutions converge as expected, with the latter solution being quite robust between $0.1 < \Delta K_{tip}/\Delta K_a < 0.9$. At high Γ, where the bridging tractions are

largest, the two solutions diverge with the parabolic solution over-predicting the dampening effect of the bridging zone.

Due to the sensitivity of the solutions to Γ, changes in test frequency and temperature (through the viscosity) would appear to be the most likely of the model variables affecting the crack-tip loading conditions in testing or service. Indeed, recent results (Miyashita et al., 1998) on elevated-temperature cyclic fatigue-crack propagation in gas-pressure sintered EC-14 silicon nitride display a marked effect of frequency (2–20 Hz) at both 1200° and 1300°C (Fig. 10). While considerations relating to applied loading frequency can be anticipated directly from the solutions presented here, it is not possible to be fully quantitative at this stage since the frequency also has a marked influence on the degree of intrinsic creep damage. Incorporating both intrinsic and extrinsic components into a crack-growth relationship for fatigue cracks in ceramics at elevated temperatures must await further modeling studies.

4. Fatigue-crack propagation in intermetallics

Due to their complex, and invariably ordered, crystal structures intermetallics generally display limited mobile dislocation activity at low homologous temperatures (below their ductile-to-brittle transition temperature, DBTT), and are thus often highly limited in ductility and toughness. To toughen intermetallics, both intrinsic and extrinsic toughening approaches have been attempted, and to varying degrees have been somewhat successful (e.g., Liu et al., 1989; Pope et al., 1995; Soboyejo et al., 1995). For example, the intermetallic compound Nb_3Al can be toughened through the addition of a ductile phase such as Nb, with the intermetallic matrix cracking preferentially to the metallic reinforcement (Murugesh et al., 1993; Cao et al., 1994; Bloyer et al., 1998). Using a high-aspect ratio reinforcement, e.g., a Nb fiber or (arrester) laminate, the crack-initiation toughness may be enhanced intrinsically by the necessity of the crack in the intermetallic matrix renucleating across the metal phase. As the crack extends and leaves a wake of uncracked Nb ligaments, the crack-growth (or R-curve) toughness may be enhanced extrinsically by crack bridging associated with a zone of intact ductile ligaments behind the crack tip.

In some respects, the mechanical behavior of intermetallics can be considered to be intermediate between metals and ceramics, ranging from compounds with some ductility, such as α_2–Ti_3Al, that display 'metal-like' characteristics, to the very brittle Ni_3Al and $MoSi_2$ that are 'ceramic-like' (below the DBTT). Specifically, with respect to fatigue-crack propagation, intrinsic damage mechanisms associated with crack advance do appear to operate in the more ductile intermetallics, as in metals. In contrast, the mechanism by which the crack extends in the cyclic fatigue of Ni_3Al and $MoSi_2$ is identical to that occurring under monotonic loads, as in ceramics (e.g., Badrinarayanan et al., 1996). Moreover, whereas the intrinsic toughening mechanisms, such as crack renucleation, do not degrade under cyclic loading, the extrinsic toughening mechanisms, such as crack bridging, can degrade severely. A notable example is ductile-phase reinforced intermetallic composites, which due to extensive crack bridging by the uncracked ductile phase can display significantly higher toughness (by a factor of 3 or greater) than the constituent matrix. However, such composite toughening is far less effective in fatigue simply because the ductile phase fails prematurely. Indeed, the fatigue-crack growth properties are often comparable, and sometimes worse, than the unreinforced matrix alloy (Venkateswara Rao et al., 1994; Murugesh et al., 1993; Badrinarayanan et al., 1996). Thus, similar to ceramic materials, cyclic loading acts to reduce the potency of extrinsic toughening mechanisms in impeding crack advance.

A good example of this behavior is shown by γ-TiAl alloys reinforced with small fractions of ductile Nb or TiNb, where toughening derives from tractions induced by unbroken ductile ligaments bridging the crack wake (Fig. 11) (Venkateswara Rao et al., 1992, 1994). For small-scale bridging, the toughness increases with crack extension up to a maximum steady-state level, K_c, associated with the development

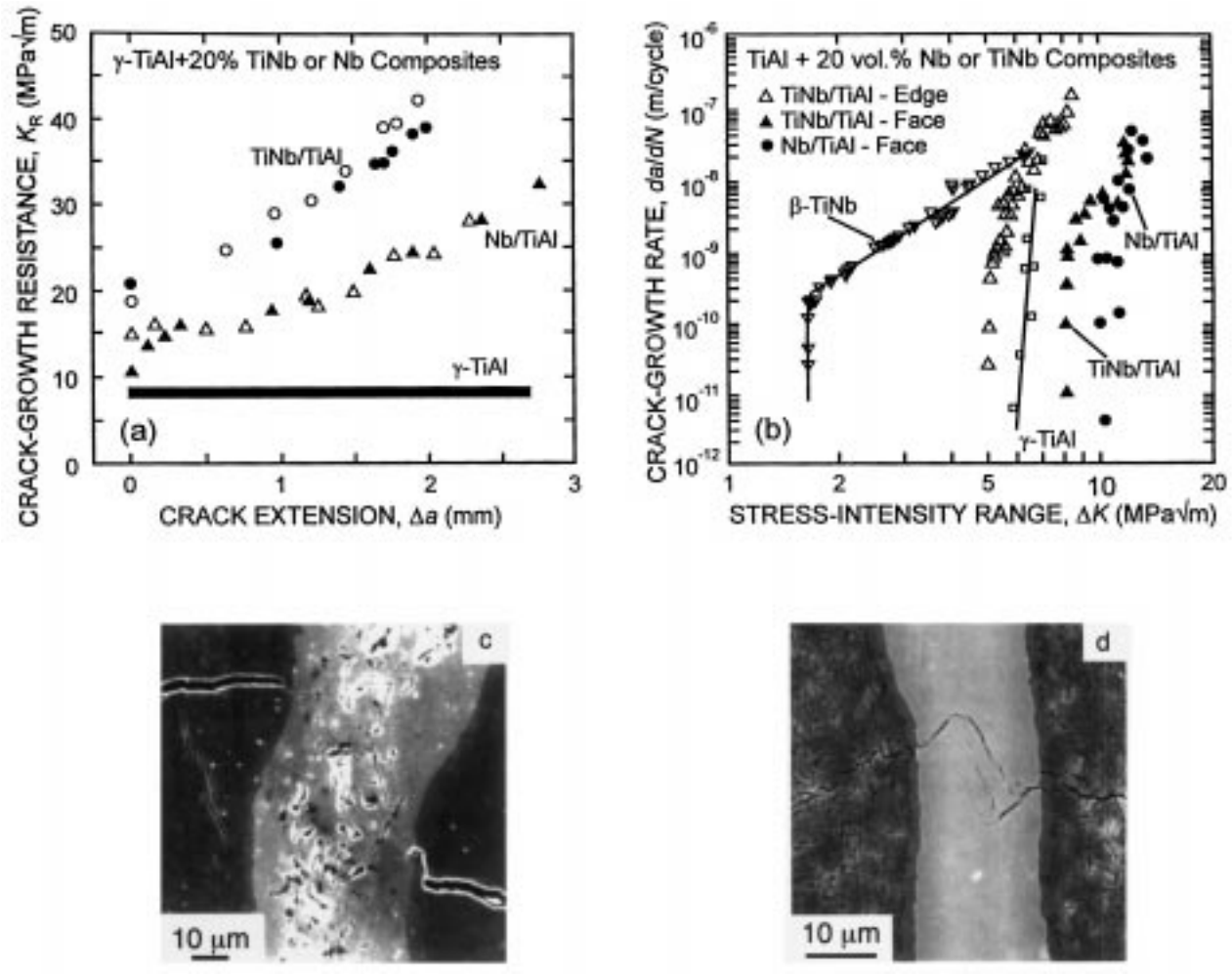

Fig. 11. (a) Fracture toughness and (b) fatigue-crack growth behavior in a 20 vol.% TiNb-reinforced γ-TiAl intermetallic composite at 25°C at $R = 0.1$ in the edge (C–R) and face (C–L) orientations. Results are compared to data for pure γ-TiAl, β-TiNb and a Nb-particulate reinforced γ-TiAl composite. (c) Extensive crack bridging by the uncracked ductile phase under monotonic loading is severely degraded under cyclic loading due to (d) premature fatigue failure of the ductile ligaments (Venkateswara Rao et al., 1992, 1994).

of a steady-state bridging zone, and can be estimated from the flow stress σ_0, volume fraction f, and size t of the reinforcement (Ashby et al., 1989):

$$K_c = \sqrt{K_t^2 + E' f t \sigma_0 \chi}, \tag{10}$$

where K_t is the critical crack-tip stress intensity at crack initiation, E' is the appropriate elastic modulus of the composite, and χ is a dimensionless function representing the work of rupture. For γ-TiAl reinforced with Nb or Nb-alloys, χ varies between 0.9 and 1.5; much larger values of χ (<4) can be obtained using strain-hardening reinforcements that debond readily from the matrix. For nominal values of $\chi = 1.2$, $\sigma_0 = 400$ MPa and $t = 100$ μm, the addition of a mere 20 vol.% of ductile particles yields

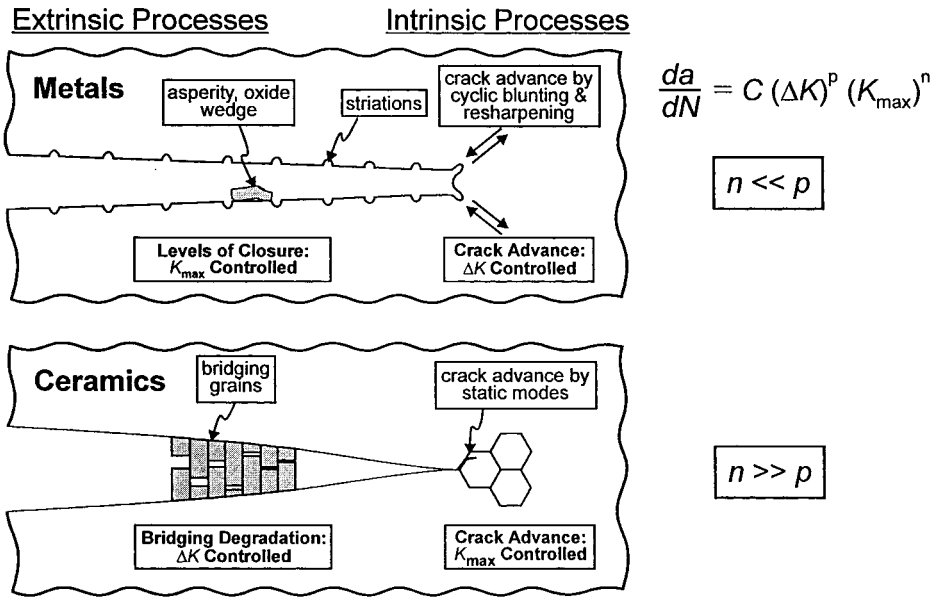

Fig. 12. Schematic illustrations of the intrinsic and extrinsic mechanisms involved in cyclic fatigue-crack growth in (a) metals and (b) ceramics, showing the relative dependencies of growth rates, da/dN, on the alternating, ΔK, and maximum K_{max}, stress intensities.

$K_c \sim 44$ MPa m^{-2}, over five times the toughness of unreinforced TiAl. Under cyclic loads, however, such bridging from unbroken ductile ligaments is compromised by the susceptibility of the ductile phase to premature fatigue failure (Venkateswara Rao et al., 1992). However, Nb reinforcements, which undergo extensive interface debonding, can delay this failure process; Nb thus provides improved fatigue resistance over reinforcements such as TiNb that are more strongly bonded to the matrix (Venkateswara Rao et al., 1994).

5. Comparison of the fatigue of ductile and brittle materials

Compared to the extensive database and understanding of fatigue failure in metals (e.g., Ritchie, 1979; Davidson and Lankford, 1992; Suresh, 1991; Ellyin, 1997), ceramics and intermetallic systems still require extensive research with respect to fatigue behavior. In such materials it is now clear that cyclic loading induces a progressive degradation in the toughening (or shielding) mechanisms behind the crack tip that locally elevates the near-tip driving force. This cyclic suppression of shielding is the principal source of the susceptibility of brittle materials to cyclic fatigue failure. By contrast, the propagation of fatigue cracks in metallic materials involves primarily *intrinsic* damage processes occurring *ahead* of the crack tip, where cracks advance by progressive blunting and resharpening of the crack tip, clearly a mechanism distinct from fracture under monotonic loads. Additionally, shielding, in the form of crack closure (wedging) mechanisms, can act in the crack wake to reduce the stress intensity range, ΔK.

Since the physical mechanisms of crack advance and crack-tip shielding are quite different in metals and ceramics, the dependencies on the alternating and mean stress intensities, specifically ΔK and K_{max}, are also quite different. A schematic illustration illustrating these differences is shown in Fig. 12. Clearly, in metals the dominant dependence of ΔK is a consequence of the intrinsic crack-advance mechanism;

the smaller K_{max} dependence results primarily from its effect of the crack-opening displacement, which in turn controls the degree of crack wedging due to crack closure in the wake. Thus, for ductile metals, $n \ll p$ in Eq. (1). In ceramics, conversely, growth rates are principally a function of K_{max}, since the crack-advance mechanism is identical to that under static loading; the much weaker ΔK dependence here arises from the cyclic-induced degradation of shielding in the wake. Thus, for ceramics, $p \ll n$. Behavior in intermetallics is generally intermediate between these two extremes.

Although both intermetallics and ceramics are susceptible to fatigue-crack growth from degradation of shielding under cyclic loads, there are significant differences. At ambient temperatures, there is no intrinsic fatigue damage mechanism in ceramics — the crack tip advances by an identical mechanism under monotonic and cyclic loads. At a given stress intensity, fatigue cracks simply grow faster due to the cyclic suppression in shielding behind the crack tip. Accordingly, the value of maximum stress intensity at the fatigue threshold, $K_{max,TH}$, is comparable with the crack-initiation toughness, K_i, at the start of the R-curve ($K_{max,TH} \sim K_i$). In many intermetallics, conversely, fatigue-crack growth is seen at stress-intensity levels far below the crack-initiation toughness, specifically $K_{max,TH} \sim 0.25$–$0.4K_I$, implying there are additional *intrinsic* microstructural damage mechanisms associated with fatigue failure. This effect is more restricted than in metals due to the limited crack-tip plasticity and consequently lower toughness of intermetallic alloys.

6. Concluding remarks

The mechanisms by which fatigue cracks grow in ductile (metals) and brittle (ceramics, intermetallic) materials are conceptually distinct. Correspondingly, any approach for microstructural design of fatigue-resistant materials must be quite different in these two classes of materials. In metals, the approach is to design microstructures that are more resistant to the intrinsic cyclic damage and that promote crack closure. In ceramics and intermetallics, the approach is to develop extrinsic toughening mechanisms that are more resilient to degradation under cyclic loads. The relevance of cyclic properties to potential applications of advanced materials is obvious, yet currently there is still uncertainty in life-prediction methodologies, only limited engineering data, and little fundamental understanding of damage, failure modes and crack-advance mechanisms. Clearly, much future effort must be devoted to this topic, particularly utilizing relevant elevated temperature and environmental conditions, if intermetallic and ceramic materials are ever to realize their potential in future structural applications.

Acknowledgements

This work was supported by the Director, Office of Science, Office of Basic Energy Sciences, Materials Sciences Division of the U.S. Department of Energy under Contract No. DE-AC03-76SF00098 (for studies on SiC), National Science Foundation under Grant No. DMR-9522134 (Al_2O_3 and Si_3N_4), and Air Force Office of Scientific Research under Grant No. F49620-96-1-0223 (intermetallics). Thanks are due to Prof. R.H. Dauskardt (Stanford University), Dr. K.T. Venkateswara Rao (Guidant Technologies), and Alexander Ziegler for their contributions to this work.

References

Ashby, M.F., Blunt, F.J., Bannister, M., 1989. Flow characteristics of highly constrained metal wires. Acta Metallurgica 37 (7), 1847–1857.

Badrinarayanan, K., McKelvey, A.L., Venkateswara Rao, K.T., Ritchie, R.O., 1996. Fracture and fatigue-crack growth behavior in ductile-phase toughened molybdenum disilicide: Effects of niobium wire vs. particulate reinforcements. Metallurgical and Materials Transactions A 27A (12), 3781–3792.

Barenblatt, G.I., 1962. The mathematical theory of equilibrium cracks in brittle fracture. Advances in Applied Mechanics 7, 55–129.

Bloyer, D.R., Venkateswara Rao, K.T., Ritchie, R.O., 1998. Fracture toughness and R-curve behavior of laminated brittle-matrix composites. Metallurgical and Materials Transactions A 29A (10), 2483–2496.

Cao, H., Löfvander, J.P., Evans, A.G., Rowe, R.G., Skelly, D.W., 1994. Mechanical properties of an *in situ* synthesized Nb/Nb_3Al layered composite. Materials Science and Engineering A 185A (1–2), 87–95.

Dauskardt, R.H., Yu, W., Ritchie, R.O., 1987. Fatigue crack propagation in transformation-toughened zirconia ceramic. Journal of the American Ceramic Society 70 (10), C248–C252.

Dauskardt, R.H., James, M.R., Porter, J.R., Ritchie, R.O., 1992. Cyclic fatigue-crack growth in a SiC-whisker-reinforced alumina ceramic composite: Long- and small-crack behavior. Journal of the American Ceramic Society 75 (4), 759–771.

Dauskardt, R.H., 1993. A frictional-wear mechanism for fatigue-crack growth in grain bridging ceramics. Acta Metallurgica et Materialia 41 (9), 2765–2781.

Dauskardt, R.H., Ritchie, R.O., 1993. Cyclic fatigue of ceramics. In: Ritchie, R.O., Dauskardt, R.H., Cox, B.N. (Eds.), Fatigue of Advanced Materials. MCEP Ltd, Edgbaston, U.K, pp. 133–151.

Davidson, D.L., Lankford, J., 1992. Fatigue crack growth in metals and alloys: Mechanisms and micromechanics. International Materials Reviews 37 (2), 45–76.

Dey, N., Socie, D.F., Hsia, K.J., 1995. Modeling static and cyclic fatigue in ceramics containing a viscous grain boundary phase. Acta Metallurgica et Materialia 43 (6), 2163–2175.

Ellyin, F., 1997. Fatigue Damage, Crack Growth and Life Prediction. Chapman & Hall, London, UK.

Evans, A.G., 1990. Perspective on the development of high-toughness ceramics. Journal of the American Ceramic Society 73 (2), 187–206.

Ewart, L., Suresh, S., 1992. Elevated-temperature crack growth in polycrystalline alumina under static and cyclic loads. Journal of Materials Science 27 (19), 5181–5191.

Foote, R.M.L., Mai, Y.-W., Cotterell, B., 1986. Crack growth resistance curves in strain-softening materials. Journal of the Mechanics and Physics of Solids 34 (6), 593–607.

Gilbert, C.J., Dauskardt, R.H., Steinbrech, R.W., Petrany, R.N., Ritchie, R.O., 1995. Cyclic fatigue in monolithic alumina: Mechanisms for crack advance promoted by frictional wear of grain bridges. Journal of Materials Science 30 (3), 643–654.

Gilbert, C.J., Cao, J.J., MoberlyChan, W.J., DeJonghe, L.C., Ritchie, R.O., 1996. Cyclic fatigue and resistance-curve behavior of an *in situ* toughened silicon carbide with Al–B–C additions. Acta Materialia 44 (8), 3199–3214.

Gilbert, C.J., Ritchie, R.O., 1997. Mechanisms of cyclic fatigue-crack propagation in a fine-grained alumina ceramic: The role of crack closure. Fatigue & Fracture of Engineering Materials & Structures 20 (10), 1453–1466.

Gilbert, C.J., Ritchie, R.O., 1998. On the quantification of bridging tractions during subcritical crack growth under monotonic and cyclic fatigue loading in a grain-bridging silicon carbide ceramic. Acta Materialia 46 (2), 609–616.

Han, L.X., Suresh, S., 1989. High-temperature failure of an alumina–silicon carbide composite under cyclic loads: Mechanisms of fatigue crack-tip damage. Journal of the American Ceramic Society 72 (7), 1233–1238.

Hay, J.C., White, K.W., 1993. Grain-bridging mechanisms in monolithic alumina and spinel. Journal of the American Ceramic Society 76 (7), 1849–1854.

Huang, C.-H., Shang, J.K., 1995. Shear-driven high-temperature fatigue crack growth in polycrystalline alumina. Acta Metallurgica et Materialia 43 (11), 4179–4187.

Irwin, G.R., 1958. Fracture. In: Handbuch der Physik, vol. 6. Springer–Verlag, Berlin, p. 551.

Kishimoto, H., Ueno, A., Kawamoto, H., Tomitaka, A., 1992. Crack propagation behavior of sintered silicon nitride under cyclic load at elevated temperature (effect of stress ratio). Journal of the Society of Materials Science, Japan 41 (471), 1805–1810 (in Japanese).

Kishimoto, H., Ueno, A., Kawamoto, H., 1995. Crack propagation behavior and mechanism of a sintered silicon nitride under cyclic load. In: Kishimoto, H., Hoshide, T., Okabe, N. (Eds.), Cyclic Fatigue in Ceramics. Elsevier, London, U.K, pp. 101–122.

Lathabai, S., Rödel, J., Lawn, B.R., 1988. Cyclic fatigue from frictional degradation at bridging grains in alumina. Journal of the Americal Ceramic Society 74 (6), 1340–1348.

Lawn, B.R., 1993. Fracture of Brittle Solids, 2nd ed. Cambridge University Press, Cambridge, U.K.

Lawn, B.R., 1998. Indentation of ceramics with spheres: A century after Hertz. Journal of the American Ceramic Society 81 (8), 1977–1994.

Liu, C.T., Taub, A.I., Stoloff, N.S., Koch, C.C. (Eds.), 1989. High-Temperature Ordered Intermetallic Alloys III, MRS Symp. Proc, vol. 133. Materials Research Society, Pittsburgh, PA.

Liu, S.-Y., Chen, I.-W., 1991. Fatigue of yttria-stabilized zirconia. I. Fatigue damage, fracture origins, and lifetime prediction. Journal of the American Ceramic Society 74 (6), 1197–1205.

Liu, S.-Y., Chen, I.-W., 1996. High temperature crack growth in silicon nitride under static and cyclic loading: Short-crack behavior and brittle–ductile transition. Acta Materialia 44 (5), 2079–2092.

Mai, Y.-W., Lawn, B.R., 1987. Crack-interface grain bridging as a fracture resistance mechanism in ceramics. II. Theoretical fracture mechanics model. Journal of the American Ceramic Society 70 (4), 289–294.

McNaney, J.M., Gilbert, C.J., Ritchie, R.O., 1999. Effect of viscous grain bridging on cyclic fatigue-crack growth in monolithic ceramics of elevated temperatures. Acta Materialia 47 (9), 2809–2819.

Miyashita, Y., Maruta, H., Hansson, T., Zhu, S., Mutoh, Y., 1998. Micromechanism of high temperature fatigue crack growth in silicon nitride. Journal of the Society of Materials Science, Japan 47 (9), 899–904.

Murugesh, L., Venkateswara Rao, K.T., Ritchie, R.O., 1993. Crack growth in a ductile-phase-toughened Nb/Nb_3Al *in situ* intermetallic composite under monotonic and cyclic loading. Scripta Metallurgica et Materialia 29 (8), 1107–1112.

Pope, D.P., Liu, C.T., Whang, S.H. (Eds.), 1995. High Temperature Intermetallics — Parts 1 & 2. Elsevier, Lausanne, Switzerland.

Ramamurty, U., Hansson, T., Suresh, S., 1994. High-temperature crack growth in monolithic and SiC_w-reinforced silicon nitride under static and cyclic loads. Journal of the American Ceramic Society 7 (11), 2985–2999.

Ramamurty, U., 1996. Retardation of fatigue crack growth in ceramics by glassy ligaments: A rationalization. Journal of the American Ceramic Society 79 (4), 945–952.

Ritchie, R.O., 1979. Near-threshold fatigue-crack propagation in steels. International Metals Reviews 20 (5–6), 205–230.

Ritchie, R.O., 1988. Mechanisms of fatigue crack propagation in metals, ceramics and composites: Role of crack tip shielding. Materials Science and Engineering A 103A, 15–28.

Rödel, J., Kelly, J., Lawn, B.R., 1990. *In situ* measurements of bridged crack interfaces in the scanning electron microscope. Journal of the American Ceramic Society 73 (11), 3313–3318.

Rouby, D., Reynaud, P., 1993. Fatigue behaviour related to interface modification during load cycling in ceramic-matrix fibre composites. Composites Science and Technology 48 (1–4), 109–118.

Soboyejo, W.O., Srivatsan, T.S., Ritchie, R.O. (Eds.), 1995. Fatigue and Fracture of Ordered Intermetallic Materials II. TMS, Warrendale, PA.

Steffen, A.A., Dauskardt, R.H., Ritchie, R.O., 1991. Cyclic fatigue life and crack-growth behavior of microstructurally small cracks in magnesia-partially-stabilized zirconia ceramics. Journal of the American Ceramic Society 74 (6), 1259–1268.

Suresh, S., 1991. Fatigue of Materials. Cambridge University Press, Cambridge, UK.

Ueno, A., Kishimoto, H., Kawamoto, H., 1992. Effects of crack size on crack propagation behavior and experimental verification of cyclic fatigue mechanism of sintered silicon nitride. In: Bradt, R.C., Hasselman, D.P.H., Munz, D., Sakai, M., Shevchenko, V.Ya. (Eds.), Fracture Mechanics of Ceramics, vol. 9. Plenum Press, New York, pp. 423–438.

Ueno, A., Kishimoto, H., Kawamoto, H., Murasawa, T., 1993. Crack propagation behavior of sintered silicon nitride under cyclic load at elevated temperature (influences of frequency and stress wave form). Journal of the Society of Materials Science, Japan 42 (479), 976–982 (in Japanese).

Van Stone, R.H., 1988. Residual life prediction methods for gas turbine components. Materials Science and Engineering A 103A, 49–61.

Venkateswara Rao, K.T., Odette, G.R., Ritchie, R.O., 1992. On the contrasting role of ductile-phase reinforcements in the fracture toughness and fatigue-crack propagation behavior of TiNb/γ-TiAl intermetallic matrix composites. Acta Metallurgica et Materialia 40 (2), 353–361.

Venkateswara Rao, K.T., Odette, G.R., Ritchie, R.O., 1994. Ductile-reinforcement toughening in gamma-TiAl intermetallic-matrix composites: Effects on fracture toughness and fatigue-crack propagation resistance. Acta Metallurgica et Materialia 42 (3), 893–911.

Wilkinson, D.S., Vitek, V., 1982. The propagation of cracks by cavitation: A general theory. Acta Metallurgica 30 (9), 1723–1732.

Yi, K.S., Cox, B.N., Dauskardt, R.H., 1999. Fatigue crack-growth behavior of materials in viscous fluid environments. Journal of the Mechanics and Physics of Solids 197 (9), 1843–1871.

Ziegler, A., McNaney, J.M., Ritchie, R.O., 1998. Subcritical crack growth in NT-164 silicon nitride at elevated temperatures. In: Vincenzini, P. (Ed.), Proceedings of the 9th CIMTEC — World Ceramics Congress and Forum on New Materials (Florence, Italy, June 14–19, 1998).